Scholarly Research Exchange

SRX Biology • Volume 2010 • Article ID 301679 • doi:10.3814/2010/301679

*Research Article*

# A Novel Mutation in Lamin A/C Gene: Phenotype and Consequences on the Protein Structure and Flexibility

**Nicola Carboni,[1] Matteo Floris,[2] Maria Valentini,[2] Giovanni Marrosu,[1] Eleonora Cocco,[1] Maria Antonietta Maioli,[1] Elisabetta Solla,[1] Anna Mateddu,[1] Marco Mura,[3] and Maria Giovanna Marrosu[1]**

[1] *Neuromuscular Unit, Department of Cardiovascular Science and Neurology, University of Cagliari, I-09100 Cagliari, Sardinia, Italy*
[2] *Bioinformatics Laboratory, CRS4, POLARIS, I-09010 Pula, Sardinia, Italy*
[3] *Dipartimento di Radiologia, Policlinico di Monserrato, Università di Cagliari, I-09100 Cagliari, Sardinia, Italy*

Correspondence should be addressed to Maria Valentini, maria@crs4.it

Received 21 October 2009; Revised 7 January 2010; Accepted 1 February 2010



Laminopathies are a heterogeneous group of *LMNA* gene alteration-related disorders including muscular dystrophies, peripheral neuropathies, progeria, lipodystrophies, mandibuloacral dysplasia and restrictive dermopathy. We recently identified a family displaying mild skeletal muscle compromise and contractures and complaining of cardiac symptoms associated to a novel mutation consisting in c.388 G/T exon 2 *LMNA* gene substitution. The aim of the study was to assess the pathogenic effect of this mutation by means of computational experiments. The c.388 G/T mutation is a missense mutation causing the substitution of the amino acid Alanine with Serine in position 130 of the protein sequence of the coiled-coil region of Lamin A rod domain. Computational predictions and molecular dynamic simulation of lamin filaments revealed a 50% reduction in the probability of the sequence adopting a coiled-coil conformation. The present study provides a feasible explanation for the potential pathogenic effect of the novel c.388 G/T exon 2 *LMNA* gene mutation. The simulation revealed how the mutation alters the flexibility of lamin filaments and likely determines an impairment in the constitution of the coiled-coil structure.

## 1. Background

Laminopathies are a group of disorders caused by alterations of the *LMNA* gene which encodes via alternative splicing for lamins of the A and C types [1]. These proteins belong to the family of type V intermediate filaments (IF) and take part in the formation of nuclear lamina, a network of protein filaments located beneath the nuclear membrane [2]. A- and C-type lamins are also present within the nucleus where they form complexes interacting with DNA, chromatin and histones [2].

Lamins feature the typical structure of IF being constituted by an N-terminal "head domain", a central alpha-helical "coiled coil" rod domain and a carboxy-terminal "tail domain" [3]. The rod domain is 350 residues long and consists of 4 alpha-helical coiled-coil segments (named 1A, 1B, 2A, and 2B) connected by means of 3 intervening regions known as *linkers* (L1, L12, and L2); it presents repeating heptads of the generalized sequence *a-b-c-d-e-f-g*, wherein *a* and *d* are predominantly apolar residues. Whilst residues involved in dimerization are usually hydrophobic, all other residues are of a hydrophilic nature [4].

*LMNA* gene contains 12 exons: exon 1 codes for N-teminal head domain and for the first portion of central rod domain, exons 2–6 code for the remaining portion of the central rod domain. Exons 7–9 yield for the sequences of carboxy-terminal tail domain portion shared by Lamin A and C, including the region of nuclear localisation signal and the portions of lamins binding directly to DNA [5]. The remaining part of tail domain is yielded by a portion of exon 10 and by exons 11 and 12 for Lamin A while by exon 10 for Lamin C. Thus, A- and C-type lamin structures differ solely in the constitution of a portion of the tail domain [5].

Numerous functions are performed by lamins, including maintaining stability of the nuclear structure, organisation of chromatin, regulation of cell cycle [6], apoptosis and various biochemical and metabolic processes [7]; they are also implicated in the regulation of gene expression, DNA replication

and mRNA transcription [8]. Lamins interact with various partners, namely, architectural partners, chromatin, partners with regulatory functions, and partners implicated in signal transduction [9].

Mutations of the *LMNA* gene determine different clinical entities including autosomal dominant and recessive Emery Dreifuss muscular dystrophy (EDMD2 and EDMD3), limb girdle muscular dystrophy 1B (LGMD 1B), dilated cardiomyopathy with cardiac conduction defects (CMD1A), progeria syndromes, lipodystrophies, mandibuloacral dysplasia, (MAD) and restrictive dermopathy (RD) [10].

It has already been demonstrated that no direct relationship can be established between *LMNA* gene mutations and clinical phenotypes and that intrafamilial and interfamilial variability in the clinical manifestations associated to the same *LMNA* gene alteration are common [11]. However, Hegele [12] and more recently Benedetti [13], showed that alterations of the *LMNA* gene are not related in a casual fashion to clinical phenotypes.

The influence of disease-related mutations on coiled-coil structures and assembly has already been discussed by means of numerous models based on computational experiments and simulation methods. Strelkov et al. [4] have modelled the structural effects of seven mutations based on the crystal structure of the lamin coil 2B fragment. The authors studied the effect of 7 mutations located at segment 2B and concluded that all mutations examined but one *(Met371Lys i*n position *f* of the heptad repeats) do not seem to interfere with dimer formation. Smith et al. [14] performed computational experiments to study the effect of amino acidic variations on the structure of cytokeratin K5/K14 proteins observed in a cohort of patients affected by epidermolysis bullosa simplex (EBS). Simulation results indicated a correlation between clinical severity of EBS and degree of structural distortion introduced by the mutation present in the coiled-coil structure; it was also shown that disruption of the coiled-coil structure was not dependent solely on whether the mutated residue lay in an inner *a/d*, adjacent *e/g*, or outer *b/c/f* position. Furthermore, using a computational model of Keratin 5 domain 1A, Liovic et al. [15] provided evidence of the effect of a conservative mutation associated to EBS on protein stability.

The above-cited studies all revealed how computational simulation may constitute a powerful tool in establishing the effect of mutations on protein structure.

In the present paper we describe a family carrying a novel *LMNA* gene mutation inherited as a dominant trait; the authors discuss the possible pathogenic mechanism of the *LMNA* gene mutation on the assembly and function of lamins by means of computational experiments including molecular dynamic simulation and predictions based on sequence conservation.

## 2. Methods

*2.1. Patients and Methods.* The proband was a 48-year-old woman with a history of rigidity of the neck and weakness of the upper limbs since her early twenties.

The fifth daughter of nonconsanguineous parents, the patient was born at term by normal vaginal delivery and grew regularly. Her past medical history included breast cancer treated by means of surgery, radio- and chemotherapy and multiple disk hernias on cervical (C4-C5 and C5-C6) and lumbar (L4-L5 and L5-S1) regions producing burning-like sensations on her shoulders, upper and lower limbs from the age of 28 to 30 years. The proband was married with one daughter and one son. Family medical history included breast cancer in three sisters, and cardiac conduction defects and peritonitis in her mother. The propositus, patients II:9 and II:13 often complained of palpitations and precordial pain.

The patient was referred to our unit at the age of 48 years; she underwent full neurological examination including MRC grading muscle strength assessment [16] and evaluation of contractures; she was also subjected to cardiological investigations including repeated standard and Holter electrocardiogrammes (ECG) and echocardiogrammes. A needle muscle biopsy from rectus femoris was performed; muscle processing, histology, and immunohystochemistry techniques were applied following indications provided by recent literature [17].

A specimen of skeletal muscle was studied by means of western blot analysis to detect proteins including dystrophin, calpain, dysferlin, sarcoglycans, and lamins that are frequently altered in the more common forms of muscular dystrophy. Western Blot was performed following the protocol indicated by Anderson and Davison [18].

Proband also underwent MRI imaging of lower limb skeletal muscle by means of a Philips Gyroscan Intera NT 1.5 T scanner equipped with a type SENSE surface coil; the protocol indicated by Mercuri et al. was followed in [19] for an appropriate evaluation of lower limb muscles. The degree of skeletal muscle compromise was measured by means of the scale proposed by Sookho et al. [20] which differentiates between mild, moderate, and severe skeletal muscle alterations.

DNA was obtained using standard methods from peripheral blood lymphocytes sampled from proband, available relatives and 100 healthy controls [21].

Analysis of *LMNA* gene for the study subject was performed by amplification and sequencing techniques. Primers for DNA amplification and sequencing were obtained using published sequence information for all exons, all intron–exon boundaries and the 5′ and 3′ untranslated regions of *LMNA*.

The coding regions of the *LMNA* gene, including the exon/intron splice sites, were amplified by PCR standard method, purified on Millipore Multiscreen filtration plates using Sephadex G-50 medium and sequenced in each direction with an ET-dye terminator cycle-sequencing system by means of the Mega BACE 1000 (Amersham Biosciences). Available relatives of the proband and 100 healthy controls were analysed by means of restriction fragment length polymorphism analysis (RFLP).

PCR products were digested with HinfI restriction enzyme and electrophoresis in 3.5% Nu Sieve.

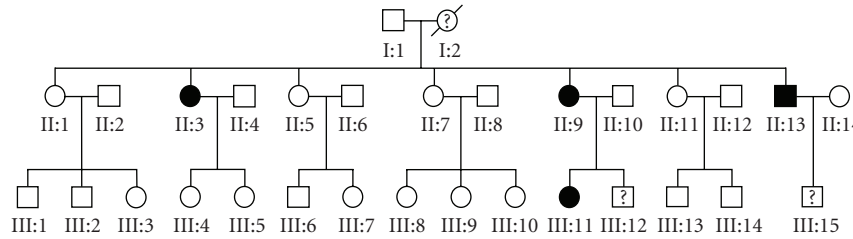


Figure 1: Pedigree of the family studied. Black square and circles indicate individuals carrying c.388 G/T exon 2 *LMNA* gene mutation.

Relatives of proband bearing *LMNA* gene mutations underwent the same clinical and instrumental investigations as propositus.

Muscle processing histology and immunohistochemistry tecniques were applied following indications provided by recent literature [17].

*2.2. Computational Methods.* To perform molecular analysis, a 3-dimensional model of the 30 residue segments surrounding the point of mutation was developed. The model was achieved by comparative modelling using the Modeller homology modelling software [22], where the sequence of the selected Lamin segment was aligned to the structure of a designed heterodimeric leucine zipper as a template.

A classical molecular dynamics (MD) approach, implemented in the NAMD program [23] using the CHARMM27 force eld with an explicit TIP3 water model [24], was applied. All simulations were performed at a temperature of 310 K (NPT ensemble); temperature and pressure control were verified by means of a Berendsen thermostat and Langevin piston. The time step used in all atomistic simulations was 1 femtoseconds. The simulations and analyses reported in this paper were performed on three model systems including model Wt (the wild-type lamin homodimer structure), model Hyb (the heterodimer formed by a mutated lamin and a wild-type chain), and finally model Mut (the mutated homodimer). The mutation p.Ala130Ser was generated on the wild-type lamin using the mutation function of Pymol software [25].

According to standard procedures, energy was initially minimised by applying 1000 steps of steepest descent energy minimization to remove possible clashing residue pairs from the initial structures. Each system was then equilibrated by 2 ps of MD runs with position restraints on the protein to allow relaxation of solvent molecules. Subsequently, MD simulation was carried out for the three systems for 4 ns.

The MATCHER program [26] was used to predict whether the sequence contained a periodically repeated pattern of amino acids. MATCHER determines whether a given protein contains the 7 residue periodicity $(a, b, c, d, e, f, g)_n$ associated with coiled-coil proteins, based on the probability of a given residue to occur on certain positions within coiled-coils.

COILS software [27] was used in quantifying the effect of the mutation on the formation of coiled-coil repeats. COILS compares a given sequence to a database of known parallel two-stranded coiled-coils and derives a similarity score. By comparing this score to the distribution of scores in globular and coiled-coil proteins, the program then calculates the probability of the sequence adopting a coiled-coil conformation.

MultiCoil program [28] was used to predict whether the mutation would lead to a shift in oligomerization state; the latter tool uses a multidimensional scoring approach to identify and distinguish trimeric and dimeric coiled coils.

ClustalW [29], a multiple sequence alignment program for DNA or proteins, was used to align the Lamin of human sequence to Lamin sequence of other vertebrates and invertebrates.

## 3. Results

*3.1. Genetic Results.* The pedigree of the family studied is illustrated in Figure 1.

Genetic analysis revealed that proband, individuals II:9, II:13 and III:11 carried a novel missense mutation consisting in substitution of Guanidine with Thymidine in position c.388 of exon 2 of the *LMNA* gene. This missense mutation was not present in unaffected relatives of the proband or in 100 healthy controls. This mutation abolishes a restriction site for Fnu4HI, creating a 175 bp fragment not present in the homozygote wild type.

*3.2. Clinical and Instrumental Finding.* Clinical and instrumental data of *LMNA* gene mutated members of this family are summarized in Table 1.

Neurological examination performed on propositus showed hypotrophy of upper limbs, bilateral winging scapulae, reduction of muscle power on shoulder girdle muscles, axial muscles and elbow flexors; evaluation of contractures evidenced severe neck rigidity, rigid spine and mild contractures of tendon Achilles (see Table 1).

On physical examination, pt II:13 appeared emaciated with scarce subcutaneous fat tissue and normal trophism; muscle power was normal for all muscle groups examined. No contractures were detected.

Physical examination of pt II:3 and pt III:11 revealed normal trophism and muscle power; evaluation of contractures showed moderate neck rigidity in both patients.

Cardiological investigations revealed mild cardiac conduction defects in the propositus, II:13 and II:3 consisting in sporadic systolic and extrasystolic beats with no alteration of heart structure or kinetics.

Table 1: Clinical and instrumental data of members of the family giving their consent for the study.

| | | Skeletal muscle involvement | | | Muscle MRI | | Cardiac compromise | | |
|---|---|---|---|---|---|---|---|---|---|
| | Age (years) | Clinical features | MRC | Contractures | Thigh's muscles | Leg's muscles | Cardiac symptoms | Echocardiogramme | Holter ECG |
| Pt II:9 | 49 | Hypotrophy on upper limbs, shoulder girdle mm weakness, winging scapulae | 3 should. flex. and abduct., 2 should. ext., 3 should adduct | Rigid spine, neck rigidity, TA (−15°) | + GG, + VV, + SEM, + LHFB | ++ MHG, ++ SO, + LHG | Palpitations; Precordial pain | Normal | SR, sporadic SVES and VES |
| Pt II:13 | 43 | Normal | N | // | // | + MHG, ++ SO, | Palpitations; precordial pain | Normal | SR, sporadic SVES |
| Pt III:11 | 21 | Normal | N | neck rigidity | + GG, + VV, + SEM, + LHFB | ++ MHG, ++ SO, + LHG | None | Normal | SR |
| Pt II:3 | 58 | Normal | N | neck rigidity | // | + MHG, ++ SO, | Palpitations; precordial pain | Normal | SR, sporadic SVES and VES |

Legend: mm, muscles; should, shoulders; flex, flexors; abduct., abductors, ext., extensors; adduct., adductors; N, normal muscle strength; TA, tendon Achilles'; +, mild alterations; ++, moderate alterations; GG, glutei muscles, VV, vasti muscles, SEM, semimembranosus, LHFB, long head of biceps femoris; MHG, medial head of gastrocnemius; LHG, lateral head of gastrocnemius; SO, soleus; SR, synusal rhythm, SVES, supraventricular systolic beats; VES, ventricular systolic beats.

MRI of lower limb skeletal muscles provided evidence of signal alterations varying from mild to moderate on soleus and medial head of gastrocnemius in the case of proband, II:3, II:13 and III;11. III:11, II:3 and II: 9; the latter also presented mild alterations of skeletal muscles of the posterior region of the thighs.

Muscle biopsy, performed on propositus, showed myopathic changes including moderate variability of fibre size and shape, rare regeneration, prevalence of type I fibres; Immunohistochemistry evidenced only a few fibres expressing foetal myosin (data not shown); it also showed normal expression and localisation of lamin A and C proteins down the nuclear membrane (Figure 5).

Protein analysis by means of western blot showed normal molecular weight and amount of proteins examined (data not shown).

*3.3. Simulation Results.* Prediction of the coiled-coil heptad-repeats along the Lamin A sequence (by means of MATCHER program) showed that the residue 130 (Alanine) is located at the *d* position in the heptad repeat.

COILS program predictions made for both the wild type and mutated lamin sequences showed a local 50% decrease in the probability of the sequence adopting a coiled-coil conformation in the segment surrounding the position 130.

No significant changes were revealed by the MultiCoil program in the probability of dimerisation (high probability score) and trimerisation (low probability score).

ClustalW alignment of the human lamin sequence with the orthologue protein of other vertebrates showed an almost complete conservation of Ala in position 130.

The ClustalW program also revealed the presence of hydrophobic residues in other aligned orthologue sequences from invertebrates. The multiple sequence alignment is shown in Figure 2.

The Molecular Dynamics experiments performed on the Wt, Hyb, and Mut structures emphasized how the average distance between the alpha carbon of the residues in position 130 is centred, respectively, around $1.0733 \pm 0.0615$ nanometers for wild type dimer, $1.0504 \pm 0.0376$ nanometers for hybrid dimer, and finally $1.120 \pm 0.038$ nanometers for the mutated dimer. The data obtained are shown in Figures 3 and 4.

## 4. Discussion and Conclusions

The case of a family characterised by contractures and varying degrees of skeletal muscle compromise complaining of cardiological symptoms is described. Clinical and instrumental investigations provided evidence of a variable compromise of skeletal muscles and extremely mild cardiac rhythm abnormalities in all mutated individuals, with the exception of pt III:11 in whom no rhythm deficits were manifested. Pt II:11 also displayed a generalised reduction of subcutaneous fat tissue.

MRI of lower limb skeletal muscles revealed mild signs of compromise in at least soleus and medial head of gastrocnemius in all affected individuals. The presence of posterior leg muscle compromise in patients carrying *LMNA* gene mutations and showing no clinical deficit of skeletal muscles has already been described [30].

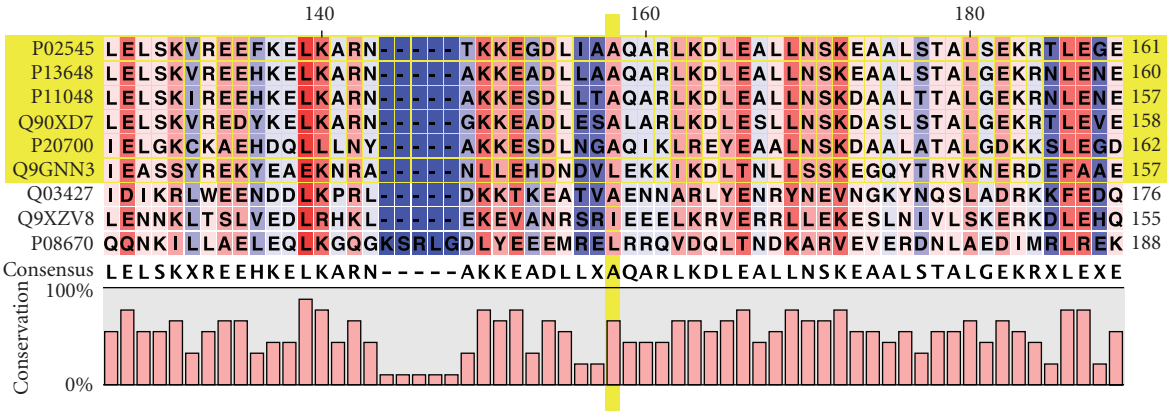


FIGURE 2: Multiple sequences alignment of Homo sapiens lamin A with orthologs. Amino acid sequence alignment of interval 104–161 of Homo sapiens lamin A/C (labelled SwissProt/TrEMBL accession number P02545) with Gallus gallus lamin A (P13648), X. laevis lamin A (P11048), zebrafish Brachydanio rerio lamin A (Q90XD7), Homo sapiens lamin B1 (P20700), Drosophila melanogaster lamin C (Q24374), worm Ciona intestinalis lamin L1 alpha (Q9GNN3), and the Hydra vulgaris lamin (Q9XZV8). For comparison, sequence of human vimentin (Vim; P08670) is also included (highlighted red). Groups of vertebrates (Ver) are highlighted in yellow. Residues are coloured by conservation. Percentage of conservation among the different sequences is shown at the bottom of the alignment.

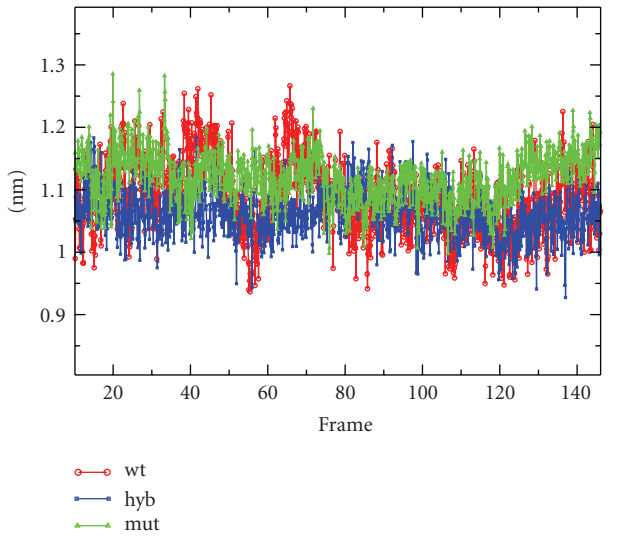


FIGURE 3: $C\alpha$ distance between mutation points monitored along the equilibrated portion of MD simulations. Distances between $C\alpha$ at position 130 for the three models of Lamin A dimer: Wt in red, Hyb in blue, and Mut in green.

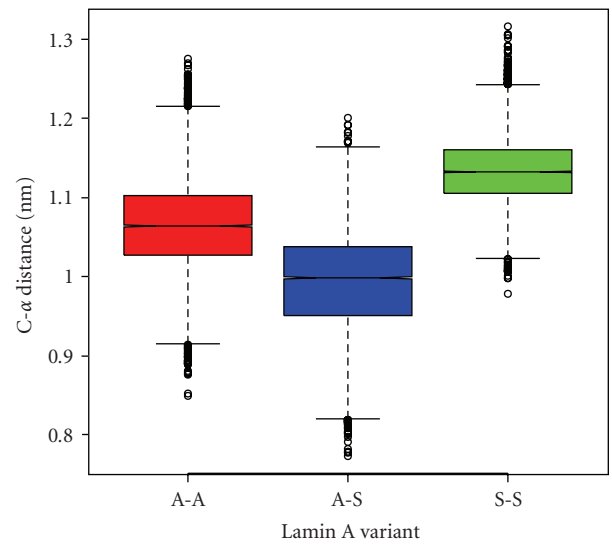


FIGURE 4: Variations in $C\alpha$ distance between mutation points on the three different dimer models. Box plot representation of variations in $C\alpha$ distance between mutation points on the three different dimer models evaluated from the equilibrated portion of MD simulation: Wt in red, Hyb in blue, and Mut in green. Hyb and Mut show a minor spread of this distance.

Genetic analysis showed that propositus, pt II:3, pt II: 13, and pt III:11 carried a novel *LMNA* gene mutation consisting in the substitution of Guanidine with Thymidine in position c.388 of exon 2.

This "base substitution" modifies the original nucleotide triplette GCT into TCT which encodes for an aminoacid Serine rather than an Alanine in position 130 of the protein sequence of the coiled-coil region of Lamin A rod domain. Since Serine and Alanine are characterised by different biochemical and structural properties, this aminoacidic variation may alter the secondary and tertiary structure of lamin filaments. Previous reports have indicated exon 2 *LMNA* gene c.357-1G > T and c.398G > T and c.398G > C as being the mutations most closely located to the one identified by our group [31].

The mutation c.357-1G > T (Asn120LeufsX5) yields for the amino acid Asparagine in the place of LeufsX5 in position 120 of lamins (described by Johan den Dunnen) whilst mutations c398G > T and c398G > C encode for an Arginine instead of a Leucine in position 133; the latter two mutations are associated to different phenotypes featuring generalized lipoatrophy, insulin-resistant diabetes,

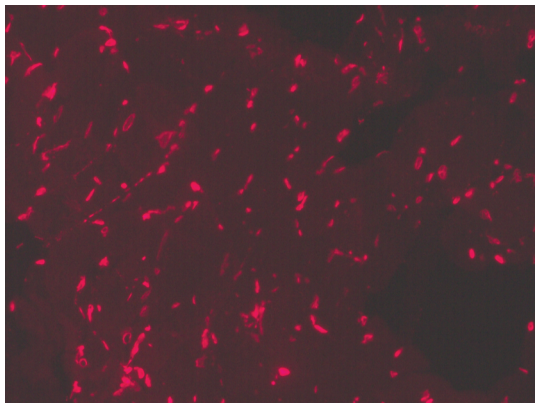

Figure 5: Immunohistochemistry of Lamin A and C protein; normal localisation of lamins of the A and C types down the nuclear membrane.

disseminated leukomelanodermic papules, liver steatosis and cardiomyopathy (mutation c398G > T) and atypical Werner's syndrome (mutation c398G > C). The reason underlying a similar diversity in clinical manifestations associated to missense mutations located in close proximity is still open to debate: modifying factors capable of explaining a diverse phenotype among individuals carrying an identical *LMNA* gene mutation or carrying *LMNA* gene mutations located at a short distance have been described previously [12].

The possible pathogenetic effect of the *LMNA* gene mutation described may be further investigated by means of computational analysis; the MATCHER program revealed a modification of flexibility and stability at the region of lamin protein in which amino acid substitution occurred.

Taking into account the *d* positions of heptads constituting the rod domain, it was evident that positions were occupied by a heterogeneous pool of amino acids featuring diverse chemical properties; indeed, analysis of the heptads predicted by MATCHER program revealed that amino acids located in *d* positions were as follows: Tyr, Leu, Val, Lys, Met, Gln, and Glu. Thus, it is feasible to maintain that substitution in position 130 of Ala, a nonpolar amino acid, with Ser, a polar amino acid, would not produce severe effects. However, comparing the multiple alignment of rod domain of human lamins with orthologue sequences of other vertebrates [4], it is noteworthy that the amino acid Ala occupying position 130 is highly conserved. This observation suggests that the presence in position 130 of an amino acid with different chemical properties is not evolutionarily favourable. The latter hypothesis is supported by predictions obtained by Coil program, based on the alignment with a database of coiled coil structures; Coil program indicates a 50% decrease in probability of obtaining a coiled-coil structure in the lamin region containing the amino acid substitution. Molecular dynamic simulations confirmed the exerting of a negative effect by Ala130Ser on rod domain stability: experiments performed provided clear evidence that the mutated homodimer is less flexible than wild type homodimer. The reduction in flexibility likely leads to an increase in dimer instability and, possibly, to an increased difficulty of interaction with lamin binding partners. A possible bias may be constituted by the current lack of knowledge on the possible binding partners interacting with mutated region of lamins.

Nevertheless, the present study demonstrates the potential utility of molecular dynamic simulations and computational experiments in clarifying the pathogenic role of a specific gene mutation.

To conclude, in the case described here, c.388 G/T exon 2 *LMNA* gene substitution was shown to cause a loss in flexibility of lamin filaments and to determine a likely impairment in the constitution of the coiled-coil structure.

## Acknowledgment

The first, the second, and the third authors contributed equally to the work.

## References

[1] D. Z. Fisher, N. Chaudhary, and G. Blobel, "cDNA sequencing of nuclear lamins A and C reveals primary and secondary structural homology to intermediate filament proteins," *Proceedings of the National Academy of Sciences of the United States of America*, vol. 83, no. 17, pp. 6450–6454, 1986.

[2] G. Bonne, "Disease associated with myonuclear abnormalities: defects of nuclear membrane related proteins (emerin, lamins a/c)," in *Structural and Molecular Basis of Skeletal Muscle Diseases*, G. Karpati, Ed., chapter 3, pp. 48–56, ISN Neuropath Press, Basel, Switzerland, 2002.

[3] S. V. Strelkov, H. Herrmann, and U. Aebi, "Molecular architecture of intermediate filaments," *BioEssays*, vol. 25, no. 3, pp. 243–251, 2003.

[4] S. V. Strelkov, J. Schumacher, P. Burkhard, U. Aebi, and H. Herrmann, "Crystal structure of the human lamin a coil 2B dimer: implications for the head-to-tail association of nuclear lamins," *Journal of Molecular Biology*, vol. 343, no. 4, pp. 1067–1080, 2004.

[5] C. A. Brown, R. W. Lanning, K. Q. McKinney, et al., "Novel and recurrent mutations in lamin A/C in patients with Emery-Dreifuss muscular dystrophy," *American Journal of Medical Genetics*, vol. 102, no. 4, pp. 359–367, 2001.

[6] B. Burke and C. L. Stewart, "Life at the edge: the nuclear envelope and human disease," *Nature Reviews Molecular Cell Biology*, vol. 3, no. 8, pp. 575–585, 2002.

[7] M. Cohen, Y. Gruenbaum, K. K. Lee, and K. L. Wilson, "Transcriptional repression, apoptosis, human disease and the functional evolution of the nuclear lamina," *Trends in Biochemical Sciences*, vol. 26, no. 1, pp. 41–47, 2001.

[8] N. M. Maraldi, C. Capanni, E. Mattioli, et al., "A pathogenic mechanism leading to partial lipodistrophy and prospects for pharmacological treatment of insulin resistance syndrome," *Acta Bio-Medica*, vol. 78, supplement 1, pp. 207–215, 2007.

[9] V. Stierlé, J. Couprie, C. Östlund, et al., "The carboxyl-terminal region common to lamins A and C contains a DNA binding domain," *Biochemistry*, vol. 42, no. 17, pp. 4819–4828, 2003.

[10] K. N. Jacob and A. Garg, "Laminopathies: multisystem dystrophy syndromes," *Molecular Genetics and Metabolism*, vol. 87, no. 4, pp. 289–302, 2006.

[11] G. Bonne, E. Mercuri, A. Muchir, et al., "Clinical and molecular genetic spectrum of autosomal dominant Emery-Dreifuss muscular dystrophy due to mutations of the lamin A/C gene," *Annals of Neurology*, vol. 48, no. 2, pp. 170–180, 2000.

[12] R. A. Hegele, "LMNA mutation position predicts organ system involvement in laminopathies," *Clinical Genetics*, vol. 68, no. 1, pp. 31–34, 2005.

[13] S. Benedetti, I. Menditto, M. Degano, et al., "Phenotypic clustering of lamin A/C mutations in neuromuscular patients," *Neurology*, vol. 69, no. 12, pp. 1285–1292, 2007.

[14] T. A. Smith, P. M. Steinert, and D. A. D. Parry, "Modeling effects of mutations in coiled-coil structures: case study using epidermolysis bullosa simplex mutations in segment 1A of K5/K14 intermediate filaments," *Proteins: Structure, Function, and Bioinformatics*, vol. 55, no. 4, pp. 1043–1052, 2004.

[15] M. Liovic, P. E. Bowden, R. Marks, and R. Komel, "A mutation (N177S) in the structurally conserved helix initiation peptide motif of keratin 5 causes a mild EBS phenotype," *Experimental Dermatology*, vol. 13, no. 5, pp. 332–334, 2004.

[16] J. John, "Grading of muscle power: comparison of MRC and analogue scales by physiotherapists," *International Journal of Rehabilitation Research*, vol. 7, no. 2, pp. 173–181, 1984.

[17] V. Dubowitz and C. Sewry, *Muscle Biopsy: A Practical Approach*, Saunders Book, St. Louis, MO, USA, 2007.

[18] L. V. B. Anderson and K. Davison, "Multiplex western blotting system for the analysis of muscular dystrophy proteins," *American Journal of Pathology*, vol. 154, no. 4, pp. 1017–1022, 1999.

[19] E. Mercuri, A. Pichiecchio, S. Counsell, et al., "A short protocol for muscle MRI in children with muscular dystrophies," *European Journal of Paediatric Neurology*, vol. 6, no. 6, pp. 305–307, 2002.

[20] S. Sookhoo, I. MacKinnon, K. Bushby, P. F. Chinnery, and D. Birchall, "MRI for the demonstration of subclinical muscle involvement in muscular dystrophy," *Clinical Radiology*, vol. 62, no. 2, pp. 160–165, 2007.

[21] J. Sambrook, E. Fritsch, T. Maniatis, et al., *Molecular Cloning*, Cold Spring Harbor Laboratory Press Cold Spring, Harbor, NY, USA, 1989.

[22] A. Sali and T. L. Blundell, "Comparative protein modelling by satisfaction of spatial restraints," *Journal of Molecular Biology*, vol. 234, no. 3, pp. 779–815, 1993.

[23] J. C. Phillips, R. Braun, W. Wang, et al., "Scalable molecular dynamics with NAMD," *Journal of Computational Chemistry*, vol. 26, no. 16, pp. 1781–1802, 2005.

[24] N. Foloppe and A. D. MacKerell Jr., "All-atom empirical force field for nucleic acids: I. Parameter optimization based on small molecule and condensed phase macromolecular target data," *Journal of Computational Chemistry*, vol. 21, no. 2, pp. 86–104, 2000.

[25] W. L. DeLano, *The PyMOL Molecular Graphics System*, DeLano Scientific, San Carlos, Calif, USA, 2002.

[26] V. A. Fischetti, G. M. Landau, P. H. Sellers, and J. P. Schmidt, "Identifying periodic occurences of a template with applications to protein structure," *Information Processing Letters*, vol. 45, no. 1, pp. 11–18, 1993.

[27] A. Lupas, M. Van Dyke, and J. Stock, "Predicting coiled coils from protein sequences," *Science*, vol. 252, no. 5010, pp. 1162–1164, 1991.

[28] E. Wolf, P. S. Kim, and B. Berger, "MultiCoil: a program for predicting two- and three-stranded coiled coils," *Protein Science*, vol. 6, no. 6, pp. 1179–1189, 1997.

[29] M. A. Larkin, G. Blackshields, N. P. Brown, et al., "Clustal W and Clustal X version 2.0," *Bioinformatics*, vol. 23, no. 21, pp. 2947–2948, 2007.

[30] N. Carboni, M. Mura, G. Marrosu, et al., "Muscle MRI findings in patients with an apparently exclusive cardiac phenotype due to a novel LMNA gene mutation," *Neuromuscular Disorders*, vol. 18, no. 4, pp. 291–298, 2008.

[31] Lamin A/C (LMNA) sequence variations, "Leiden Muscular Dystrophy pages," 2008, http://www.dmd.nl/.